Supporting Information

Multi-piezo Effects and Ferroelectricity in a Two-Dimensional Multiferroic Altermagnet Ti_2Se_2S

M. Abaker [a, b], Naveed Ullah [c, *], Arshad Khan [a, b], Jawed Mustafa [c]

[a] Department of Physics, Faculty of Arts and Sciences, Najran University, Najran, Saudi Arabia

[b] Advanced Materials and Nano Research Center (AMNRC), Najran University, P.O. Box: 1988, Najran 11001, Saudi Arabia

[c] Department of Mechanical Engineering, College of Engineering, King Faisal University, Al-Ahsa, 31982, Saudi Arabia

* Corresponding Email: Naveedullah@kfu.edu.sa

Neel temperature

The magnetic transition temperature of Ti_2Se_2S monolayer was evaluated from atomistic spin dynamics simulations by analyzing the evolution of the sublattice magnetization as a function of temperature using the VAMPIRE code. The magnetic interactions were described through the classical Heisenberg Hamiltonian with an additional uniaxial anisotropy term [1],

$$H_{ex} = -\sum_{i \neq j} J_{ij}(S_i \cdot S_j) - k_u(S_i \cdot e)^2 \quad (1)$$

where J_{ij} denotes the magnetic exchange coupling between spins located at sites i and j, S_i and S_j are unit vectors representing the local spin directions, k_u is the magnetic anisotropy constant, and e defines the easy axis of magnetization. The normalized magnetization of each magnetic sublattice was obtained from

$$n_\alpha = \frac{1}{N_\alpha}\sum_{i}^{N_\alpha} S_i \quad (2)$$

where N_α is the number of magnetic atoms belonging to sublattice α. The exchange parameter was estimated from the energy difference between the ferromagnetic and antiferromagnetic configurations according to $J_{ij} = \frac{E_{ex}}{Nm^2}$ where E_{ex} is the magnetic exchange energy, N is the number of magnetic atoms in the unit cell, and m is the local magnetic moment. The temperature dependent magnetic behavior was investigated using the field cooling protocol implemented in VAMPIRE together with the Landau Lifshitz Gilbert dynamics solved by the Heun integration scheme. A 50 × 50 × 1 magnetic supercell with periodic boundary conditions was employed to minimize finite size effects. Each simulation consisted of 1.0×10^6 integration steps to ensure reliable statistical averaging. The calculated sublattice magnetization curve n(T) for Ti_2Se_2S monolayer is presented in SI Figure S1. The simulation data are represented by blue symbols, while the blue curve corresponds to a fit based on the critical behavior expression $n(T) = \left[1 - \frac{T}{T_N}\right]^\beta$ using a critical exponent of β = 0.38. We obtained the Neel temperature (T_N) of approximately 250 K. This value is close to room temperature, indicating that the antiferromagnetic ordering in the Ti_2Se_2S monolayer remains stable over a broad temperature range. Such a relatively high Neel temperature is advantageous for practical device operation and suggests that Ti_2Se_2S could be a promising candidate for near room temperature antiferromagnetic spintronic applications.

Spin Hall conductivity

To further elucidate the spin transport characteristics of the Ti_2Se_2S monolayer, we calculated the intrinsic spin Hall conductivity (SHC) for the pristine system as well as under ±4% uniaxial strain along the X direction. The SHC was evaluated within the framework of the Kubo linear response theory. The intrinsic SHC tensor is given by [2, 3]

$$\sigma_{\alpha\beta}^{spin\,\gamma} = -\frac{e^2}{\hbar V N_k}\frac{1}{\sum_k \Omega_{\alpha\beta}^{spin\,\gamma}(k)} \quad (3)$$

$$\Omega_{\alpha\beta}^{spin\,\gamma}(k) = \sum_{n} f_{nk}\Omega_{n\,\alpha\beta}^{spin\,\gamma}(k) \tag{4}$$

$$\Omega_{n,\alpha\beta}^{spin\,\gamma}(k) = \hbar^2 \sum_{m \neq n} \frac{-2Im\left\langle nk\left|\frac{1}{2}\{\hat{\sigma}_\gamma, \hat{v}_\alpha\}\right|mk\right\rangle\langle mk|\hat{v}_\beta|nk\rangle}{(E_{nk} - E_{mk})^2} \tag{5}$$

Here, f_{nk} represents the Fermi-Dirac distribution function, and $v_{\alpha,\beta}$ denote the velocity operators. Furthermore, n and k represent the periodic part of the Bloch wave function with Eigenvalue E_{nk}, V is the primitive cell volume, and N_k denotes the number of k-points in the Brillouin zone [1]. A set of maximally localized Wannier functions (MLWFs) was constructed from the Bloch wave function obtained from density functional theory. The calculated SHC as a function of chemical potential (μ) is presented in SI Figure S2 (a) – (c) for +4% strained, pristine, and −4% strained systems. Two spin current channels were considered, namely SHC; $\sigma_{zy}^{spin\,x}$ and $\sigma_{zx}^{spin\,y}$ corresponding to spin polarization along the X and Y directions, respectively. For the pristine system, both SHC components are nearly zero at the Fermi level (μ=0 eV), which is consistent with the semiconducting electronic structure. Around the valence band region, $\sigma_{zy}^{spin\,x}$ exhibits a pronounced negative peak reaching approximately -60 ($\hbar$/e)S/cm near μ ≈ -0.7 eV, whereas $\sigma_{zx}^{spin\,y}$ shows a much smaller response. In the conduction band region, both SHC components remain relatively weak with magnitudes below about 10 ($\hbar$/e)S/cm.

Under a compressive strain of -4%, the SHC is significantly enhanced in the hole doped region. The $\sigma_{zy}^{spin\,x}$ component reaches a maximum value of approximately 70 ($\hbar$/e)S/cm around μ ≈ -0.8 eV, while $\sigma_{zx}^{spin\,y}$ exhibits a comparable positive peak of about 45 ($\hbar$/e)S/cm. In contrast, the electron doped region displays a relatively weak response. Notably, the two SHC components possess opposite signs near the Fermi level, reflecting the anisotropic spin Berry curvature distribution induced by the altermagnetic electronic structure. In contrast, tensile strain (+4%) strongly suppresses the overall SHC magnitude. The $\sigma_{zy}^{spin\,x}$ component remains close to zero throughout most of the investigated energy range, with only a small

negative feature near μ ≈ -0.6 eV. However, $\sigma^{spin\,y}_{zx}$ exhibits a sharp positive peak reaching approximately 16 ($\hbar$/e)S/cm near μ ≈ -0.6 eV. Away from this localized feature, both SHC components remain relatively small. Overall, the results demonstrate that the spin Hall response of the Ti_2Se_2S monolayer is highly sensitive to strain engineering. Compressive strain substantially enhances the spin Hall conductivity, particularly in the hole doped regime, whereas tensile strain suppresses the SHC. The opposite signs observed for $\sigma^{spin\,x}_{zy}$ and $\sigma^{spin\,y}_{zx}$ near the Fermi level further indicate a pronounced anisotropic spin transport behavior originating from the strain dependent redistribution of spin Berry curvature in momentum space. Such tunable SHC characteristics highlight the potential of the Ti_2Se_2S monolayer for strain controlled spintronic applications.

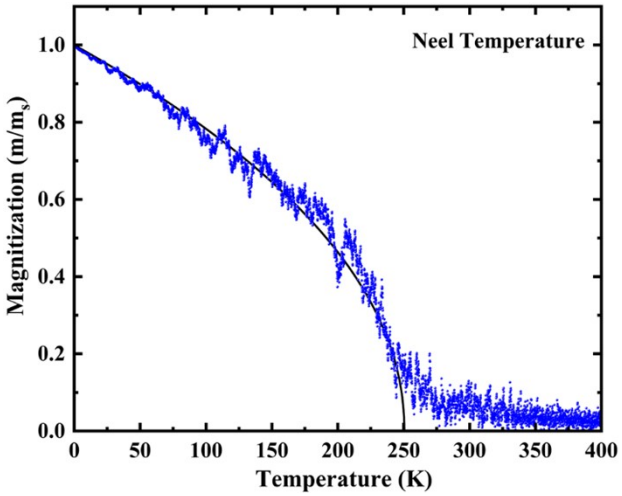

Figure S1. Temperature dependent normalized magnetization(m/m_s)obtained from Monte Carlo simulations, showing a magnetic phase transition with a Neel temperature (T_N) of approximately 250 K.

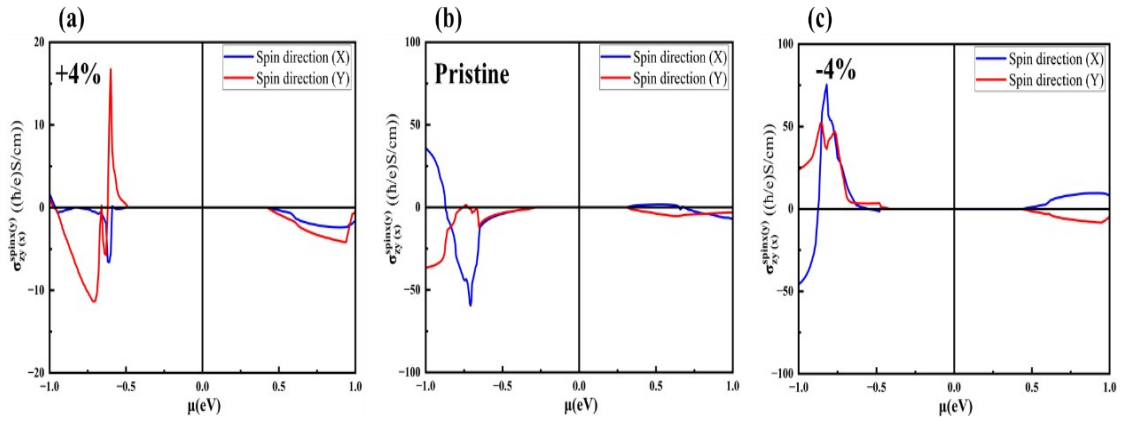

Figure S2. Spin Hall conductivity as a function of chemical potential (μ) for (a) +4% tensile strain, (b) the pristine system, and (c) -4% compressive strain.

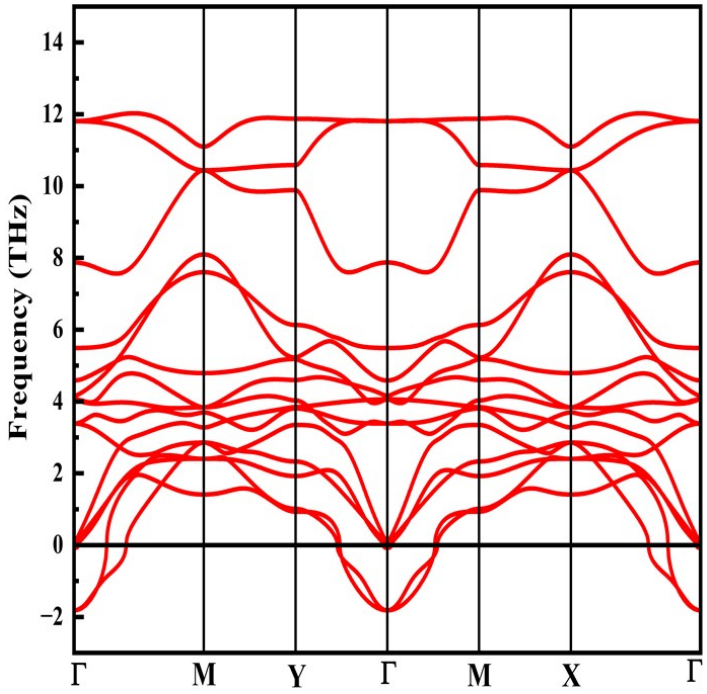

Figure S3. Phonon dispersion of the intermediate centrosymmetric state. The imaginary phonon modes around the Γ point confirm the dynamical instability of the nonpolar configuration and support the ferroelectric nature of the Ti_2Se_2S monolayer.

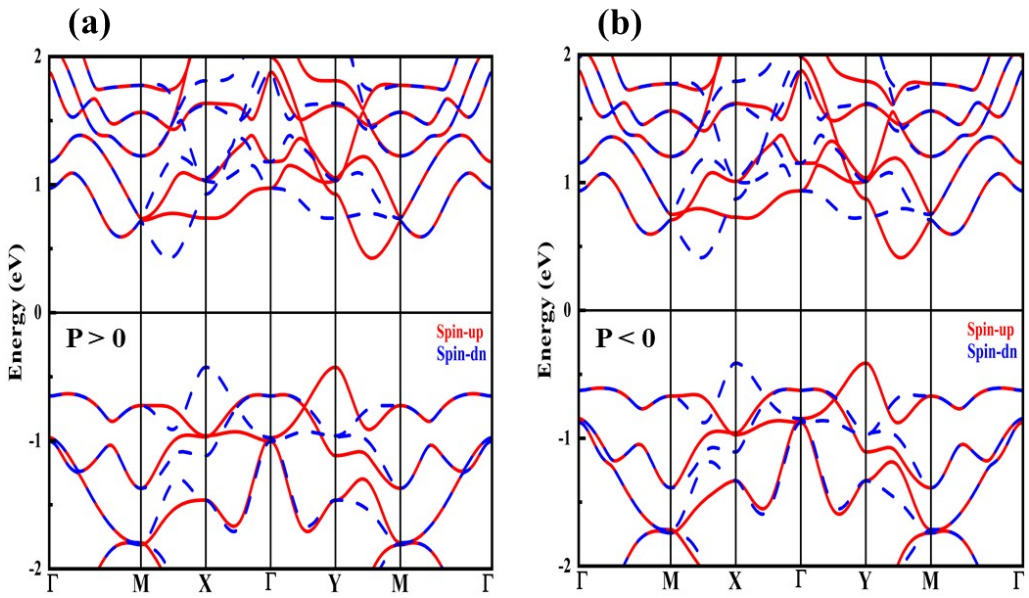

Figure S4. Electronic band structures of the ferroelectric states with positive (P > 0) and negative (P < 0) polarization. The spin resolved band structures show nearly identical electronic dispersions and altermagnetic spin splitting for both polarization states, indicating that polarization reversal has a negligible effect on the electronic structure. This result suggests that the altermagnetic state is preserved during ferroelectric switching. Red and blue lines represent the spin up and spin down bands, respectively.

```
POSCAR-Ti2Se2S
   1.00000000000000
      4.5167085377896816    0.0000000000000000    0.0000000000000000
      0.0000000000000000    4.5167085377896816    0.0000000000000000
      0.0000000000000000    0.0000000000000000   25.0000000000000000
      Ti   Se   S
       2    2    1
Direct
        0.0000000000000000  0.5000000000000000  0.5293578704542065
        0.5000000000000000 -0.0000000000000000  0.5293578704542065
        0.0000000000000000 -0.0000000000000000  0.4645726136967505
        0.0000000000000000 -0.0000000000000000  0.5975330079054429
        0.5000000000000000  0.5000000000000000  0.4963518104524998
```

Figure S5. Optimized POSCAR file of the Ti_2Se_2S monolayer containing the lattice vectors, atomic composition, and fractional atomic coordinates of the fully relaxed structure.

References

1 Zeng, H., Zhang, W., Zhao, J., & Ding, D. (2026). Crystal symmetry paired spin-valley locking in the monolayered K 2 V 2 Se 2 O altermagnet. *Physical Review B*, *113*(10), 104405.

2 Qiao, J., Zhou, J., Yuan, Z., & Zhao, W. (2018). Calculation of intrinsic spin Hall conductivity by Wannier interpolation. *Physical Review B*, *98*(21), 214402.

3 Jeong, D., Kang, S. H., & Kwon, Y. K. (2026). Magnetic and crystal symmetry control on spin Hall conductivity in altermagnets. *Advanced Science*, *13*(13), e15002.